



OPEN

Impairments in the early consolidation of spatial memories via group II mGluR agonism in the mammillary bodies

Michal M. Milczarek , James C. Perry , Eman Amin, Salma Haniffa , Thomas Hathaway & Seralynne D. Vann ✉

mGluR2 receptors are widely expressed in limbic brain regions associated with memory, including the hippocampal formation, retrosplenial and frontal cortices, as well as subcortical regions including the mammillary bodies. mGluR2/3 agonists have been proposed as potential therapeutics for neurological and psychiatric disorders, however, there is still little known about the role of these receptors in cognitive processes, including memory consolidation. To address this, we assessed the effect of the mGluR2/3 agonist, eglumetad, on spatial memory consolidation in both mice and rats. Using the novel place preference paradigm, we found that post-sample injections of eglumetad impaired subsequent spatial discrimination when tested 6 h later. Using the immediate early gene *c-fos* as a marker of neural activity, we showed that eglumetad injections reduced activity in a network of limbic brain regions including the hippocampus and mammillary bodies. To determine whether the systemic effects could be replicated with more targeted manipulations, we performed post-sample infusions of the mGluR2/3 agonist 2R,4R-APDC into the mammillary bodies. This impaired novelty discrimination on a place preference task and an object-in-place task, again highlighting the role of mGluR2/3 transmission in memory consolidation and demonstrating the crucial involvement of the mammillary bodies in post-encoding processing of spatial information.

Memory formation is a complex process, involving encoding, consolidation, and recall. These processes depend on a network of brain regions whose relative contribution varies according to memory stage as well as its content. The medial diencephalon, including the mammillary bodies, has long been implicated in memory processing^{1–3}, especially in relation to encoding^{4–7}. By contrast, less is known about its possible contributions to consolidation, which has been more closely aligned with the medial temporal lobe and cortical regions^{8,9}, which are sites directly involved in memory storage. However, increasing evidence suggests an active role for subcortical regions in orchestrating systems-wide memory consolidation, via neuromodulatory inputs^{10,11} and generation of oscillatory activity¹². This role may be extended to the mammillary bodies given their importance for arousal and coordinating hippocampal-network activity^{2,13}.

The mammillary bodies form part of an extended memory system (the Papez network), receiving their major glutamatergic input from the subiculum via the postcommissural fornix and projecting to the anterior thalamic nuclei, which in turn reciprocally connect with the hippocampal formation and cortical regions involved in mnemonic processing¹⁴. Mammillary body activity is modulated via their reciprocal connections with Gudden's tegmental nuclei, and inputs from the septum and supramammillary nuclei². This enables the mammillary bodies to modulate and amplify relevant signals for subsequent processing in downstream regions^{2,13}, in addition, their role in the propagation of sharp-wave ripple-related activity¹⁵ provides a further mechanism via which the mammillary bodies may contribute to consolidatory processes¹⁶.

The mammillary bodies show evidence of highly specialized glutamatergic transmission: they express vesicular glutamate transporters as well as ionotropic and metabotropic glutamate receptors^{17,18}. Indeed, the medial mammillary nucleus has some of the highest metabotropic glutamate receptor 2 (mGluR2) expression levels, along with other regions in the Papez network including the hippocampus, and retrosplenial cortex¹⁹. The distribution of mGluR2 in the brain might suggest that modulating mGluR2 activity would impact memory processes. However, the effects of mGluR2/3 agonists on spatial working memory tasks appear mixed²⁰, with some studies

School of Psychology & Neuroscience and Mental Health Innovation Institute, Cardiff University, 70 Park Place, Cardiff CF10 3AT, UK. ✉email: vannsd@cardiff.ac.uk

finding impairments^{21,22} while others showing improvements²³ and others showing no effect on cognition²⁴. However, metabotropic glutamate receptors in general have also been implicated in memory consolidation²⁵, due to their role in slower, longer-lasting modulatory effects²⁶, including long-term depression²⁷, and mGluR2 could therefore be mediating consolidatory processes within the Papez network²⁸.

To assess the effects of mGlu2/3 receptor manipulation on early consolidation processes, rats and mice were systemically injected with an mGluR2/3 agonist, eglumetad (LY354740), immediately after the sample phase of a novel place preference task and a discrimination test was carried out after a 6-h delay. A motility test was used to determine whether the injections had any overall effects on activity. To identify which brain regions were affected by systemic eglumetad injections, we quantified the expression of the immediate early gene *c-fos* across the Papez network in mice that had explored a novel environment after receiving either an injection of eglumetad or saline.

The next step was to determine whether the systemic effects of mGlu2/3 agonists could be replicated with more targeted administration and for this we looked at the effects of mGlu2/3 receptor agonism in the mammillary bodies. The mammillary bodies were selected as they have particularly high levels of mGlu2 receptor expression¹⁹ and slice studies have shown the mGluR2/3 agonist, APDC, to inhibit mammillary body activity²⁹. Animals were tested on two spatial discrimination tasks that assess incidental learning and rely on an animal's innate preference for novelty³. By looking at spatial discrimination behavior with a 6-h delay, and administering the drug post-sample, it was possible to study the impact of an mGluR2/3 agonist on early consolidation while leaving the animals unaffected by any acute effects of the drug during both encoding and recall periods.

Results

Experiment 1

We first tested the impact of eglumetad injections in rats on open field exploration and found no effect on total distance travelled, mean distance from the center of the arena or time spent in the centre of the arena at 30 min post-injection (total distance travelled: $t = -0.34$, $p = 0.63$, $d = -0.09$; mean distance from center: $t = 0.09$, $p = 0.46$, $d = 0.02$; time in the center of the maze: $t = 0.51$, $p = 0.7$, $d = 0.14$; Fig. 1 a–c; Fig. S1a) or at 6 h post-injection (total distance travelled: $t = 1.41$, $p = 0.09$, $d = 0.37$; mean distance from center: $t = -0.98$, $p = 0.84$, $d = -0.26$; time in the center of the maze: $t = 0.6$, $p = 0.73$, $d = 0.16$; Fig. S1b–e; one-sided within-subject permutation tests).

Next, we investigated the effect of the drug on memory consolidation using the novel place preference (NPP) task with a 6 h delay between sample and test. Post-sample injections of eglumetad impaired novel spatial discrimination (Fig. 1d), as demonstrated by a significant reduction in cumulative discrimination scores when compared with saline injections ($t = 1.79$, $p = 0.047$, $d = 0.55$; one-sided within-subject permutation test; Fig. 1e,f). Furthermore, rats displayed clear novel place preference with above-chance cumulative discrimination scores following saline injections ($t = 3.59$, $p = 1.62 \times 10^{-3}$; one-sided within-subject permutation test) whereas they performed at chance following eglumetad injections ($t = 1.02$, $p = 0.16$). The differences in discrimination were not driven by changes in general activity as there was no effect of drug on total number of arm entries or mean duration of time spent in the arms either at sample or test phases of the task (number of entries at sample: $t = -0.97$, $p = 0.38$, $d = -0.21$; mean arm visit time at sample: $t = 0.63$, $p = 0.54$, $d = -0.14$; number of entries at test: $t = 0.06$, $p = 1$, $d = 0.012$; mean arm visit time at sample: $t = 0.68$, $p = 0.51$, $d = -0.15$; two-sided within-subject permutation tests). However, we found that total active exploration at sample was negatively correlated with subsequent discrimination scores at test following saline injections ($r = -0.56$, $p = 0.024$) but not following eglumetad injections ($r = -0.04$, $p = 0.88$). We therefore tested if inclusion of sample total exploration data improved the estimation of discrimination scores at test and found that it marginally did ($\lambda = 3.88$, $p = 0.049$, compared to a model lacking sample data), while still returning the main effect of drug ($F_{1,29} = 5.45$, $p = 0.027$) and a trend for sample total exploration on D2 scores at test ($F_{1,29} = 4.13$, $p = 0.051$).

We also measured the concentration of the drug in rat brains at increasing intervals between 10 and 360 min from injection, confirming its presence immediately after injection and a near full wash-out by 6 h (5.5-fold decrease, Fig. S2).

Experiment 2

As with rats (Experiment 1), eglumetad injections had no effect on the total distance travelled in the open field in mice ($t = 0.44$, $p = 0.33$, $d = 0.18$; one-sided between-subject permutation test; Fig. 2a,b). However, unlike the effect on rats, the injections in mice resulted in greater exploration in the center of the arena as measured by mean distance from center ($t = 2.59$, $p = 9.93 \times 10^{-3}$, $d = 1.03$, one-sided between-subject permutation test; Fig. 2a,c) but not when using the time spent in center of the arena ($t = 1.24$, $p = 0.12$, $d = 0.55$; Fig. S3).

Eglumetad affected performance on the NPP task in mice (Fig. 2d) in the same way as in rats, with saline-injected mice displaying above-chance discrimination ($t = 4.6$, $p = 9.77 \times 10^{-4}$) and eglumetad-injected mice showing no preference ($t = 1.43$, $p = 0.090$; one-sided between-subject permutation tests, Fig. 2e–f). This was reflected in significant drug-related differences in discrimination scores ($t = 1.85$, $p = 0.038$, $d = 0.69$, one-sided between-subject permutation test). The impaired discrimination following eglumetad injections did not reflect changes in overall activity as there was no effect of drug on the number of arm entries and the mean duration of time spent in the arms at either sample or test phases of the task (number of entries at sample: $t = -1.19$, $p = 0.23$, $d = -0.44$; mean arm visit time at sample: $t = 2.07$, $p = 0.050$, $d = -0.77$; number of entries at test: $t = 0.016$, $p = 0.98$, $d = 0.006$, mean arm visit time at test: $t = -0.45$, $p = 0.67$, $d = 0.17$, two-sided permutation tests). As with rats, we found total sample exploration time to negatively correlate with subsequent discrimination at test, this time both for saline ($r = -0.58$, $p = 0.0490$) and eglumetad ($r = -0.56$, $p = 0.0495$). Inclusion of sample exploration data significantly improved the mixed effects model ($\lambda = 7.91$, $p = 0.0049$), still returning a main effect of drug ($F_{1,22} = 9.33$, $p = 0.0058$) and a main effect of total exploration ($F_{1,22} = 9.3$, $p = 0.0059$). Factoring in sex did not improve the model ($\lambda = 0.007$, $p = 0.92$), suggesting the effect of the drug was equivalent in males and females.

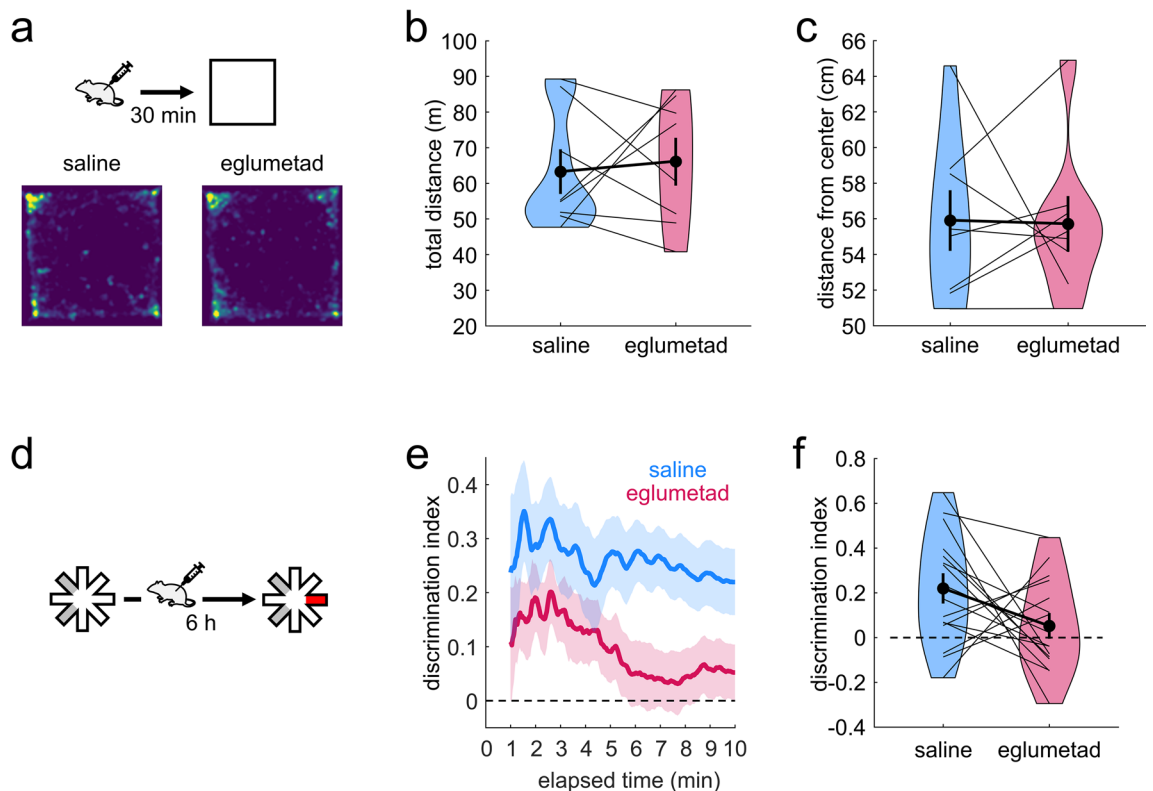


Figure 1. The effect of eglumetad on open field activity and novel place preference in rats. **(a)** Schematic representation of the open field task and heatmaps representing mean arena occupancy ($n = 8$, within-subject design). **(b)** Violin plot of total distance travelled. The vertical bars are standard error of the mean, black dots represent the means, thin lines connect data from individual animals and the bolded line connects the means. **(c)** Violin plot of the mean distance from center of the open field. Lower values suggest less anxiety. **(d)** Schematic representation of the novel place preference task ($n = 16$, within-subject design): rats were presented with two sample maze arms for 10 min, followed by intraperitoneal injections and 6 h later given access to three arms (one novel and two familiar) for 10 min. The discrimination index at test was calculated as the ratio of the difference in time spent in the novel and familiar arms and the summed time spent in the novel and familiar arms. **(e)** Timeline of the cumulative discrimination index following saline or eglumetad injections. The solid lines represent mean values and the shaded areas, the standard error of the mean. **(f)** Violin plot of mean discrimination indices, calculated over 10 min of maze exploration at test. The horizontal line in **(e)** and **(f)** denotes chance-level performance.

Experiment 3

To identify which brain areas were affected by systemic eglumetad injections (10 mg/kg), we looked at the effects of the drug on novelty-induced *c-fos* expression across limbic brain regions in mice. Mice were injected with either eglumetad or saline 30 min before being placed in a novel environment. While eglumetad injections had no effect on motility ($t = 0$, $p = 0.68$, $d = -0.23$; one-sided between-subject permutation test; Fig. 3a,b), *c-fos* levels showed a marked reduction across multiple limbic areas. A mixed effect model ('Density~Drug × Region + (1|Animal)') returned a main effect of drug ($F_{1,11} = 9.32$, $p = 2.72 \times 10^{-3}$), a main effect of region ($F_{1,11} = 13.94$, $p = 4.86 \times 10^{-20}$) and a drug × region interaction ($F_{14,154} = 1.83$, $p = 0.039$; Fig. 3c,d). Pairwise comparisons revealed significant differences in all regions of interest apart from the visual cortex, postsubiculum, anteroventral and anteromedial thalamic nuclei (Fig. S4).

Experiment 4

Experiment 3 identified several limbic regions that were affected by eglumetad injections. Among these, the mammillary bodies show high levels of circumscribed mGluR2 expression (Fig. 4e) and they have also been shown to directly respond to group II metabotropic agonism²⁹. As such, we hypothesized that local infusion of mGluR2/3 agonists into the mammillary bodies would be sufficient to impair spatial memory consolidation.

To test this, we cannulated 45 rats to locally infuse the mGluR2/3 agonist, 2R, 4R-APDC (Fig. 4a). Postmortem validation, including cresyl (Fig. 4d) and DAB staining (Fig. S5b for individual subjects), and in some cases, infusions of a fluorescent dye (Fig. 4f), confirmed correct cannula placement, with limited tissue damage, in 26 rats (Fig. 4b,c and Fig. S5a). To ensure local infusions of APDC had no effect on motility, the rats were tested on open field exploration following saline and APDC infusions. There was no effect of drug on total distance travelled ($t = -1.01$, $p = 0.83$, $d = -0.26$) or mean distance from the center of the arena ($t = 1.5$, $p = 0.090$, $d = 0.39$)

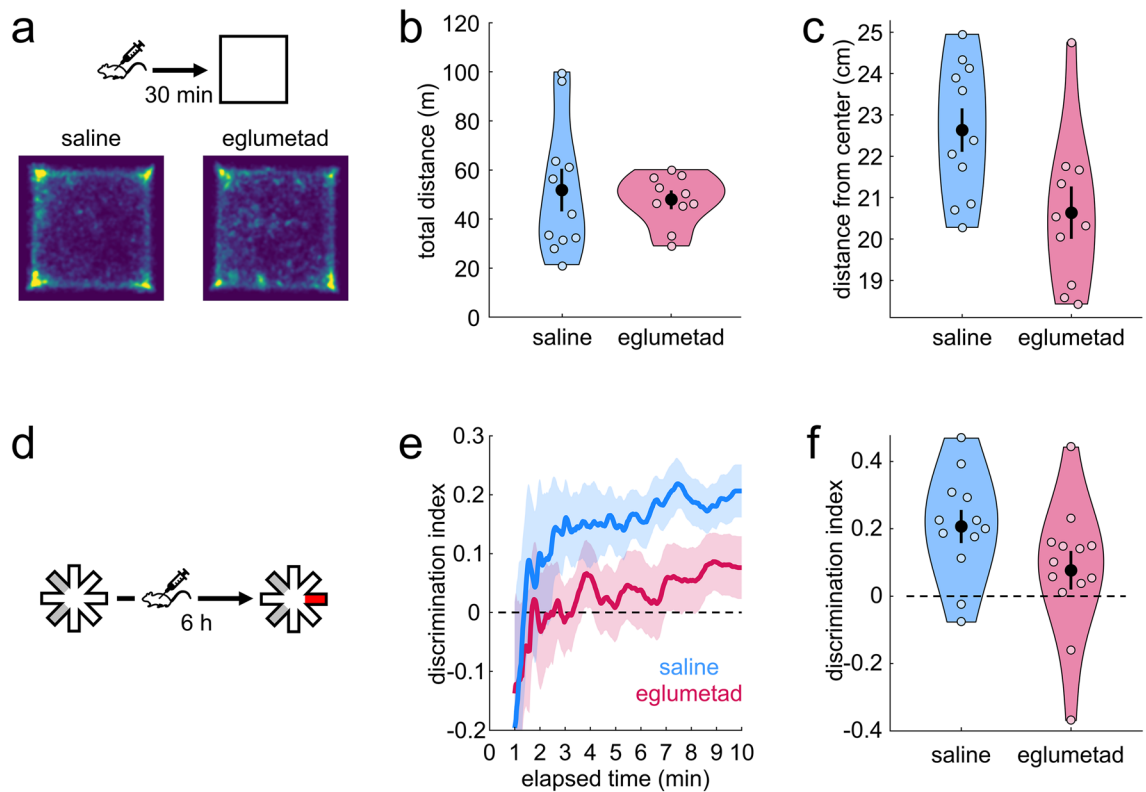


Figure 2. The effect of eglumetad on open field activity and novel place preference in mice. (a) Schematic representation of the open field task and heatmaps representing mean arena occupancy (saline: seven female, four male; eglumetad: four female, six male). (b) Violin plot of total distance travelled, as in Fig. 1 b. (c) Violin plot of the mean distance from center of the open field. Lower values signify less anxiety. (d) Schematic representation of the novel place preference task. (e) Timeline of the cumulative discrimination index in mice that received saline (blue: five female; seven male) or eglumetad (red: five female; eight male) following sample. The solid lines represent mean values and the shaded areas, the standard error of the mean. (f) Violin plot of mean discrimination indices, calculated over 10 min of maze exploration at test. The horizontal line in (e) and (f) denotes chance-level performance.

but a trend for increased time spent in the center of arena ($t = 1.96$, $p = 0.055$, $d = 0.51$, one-sided within-subject permutation tests; Fig. 5a–c, Fig S6).

For the NPP task (Fig. 5d), we found a similar pattern to that of the systemic injection experiments, with APDC infusions leading to significantly lower discrimination scores compared to saline infusions ($t = 3.06$, $p = 5.08 \times 10^{-3}$, $d = 0.54$, one-sided within-subject permutation test; Fig. 5e,f). However, unlike the systemic injections, rats' performance was above chance following both saline ($t = 6.38$, $p = 6.1 \times 10^{-5}$) and APDC infusions ($t = 2.07$, $p = 0.03$; one-sided within-subject permutation tests), showing rats could discriminate the novel arm under both drug conditions. The main effect of drug was not driven by differences in overall activity levels at either sample or test (number of entries at sample: $t = -0.32$, $p = 0.81$, $d = -0.074$; mean arm visit time at sample: $t = 1.08$, $p = 0.30$, $d = -0.25$; number of entries at test: $t = -0.20$, $p = 0.89$, $d = -0.05$, mean arm visit time at test: $t = -0.12$, $p = 0.91$, $d = 0.028$; two-sided within-subject permutation tests). There were no relationships between sample exploration times and discrimination at test (saline: $r = 0.0033$, $p = 0.99$, APDC: $r = 0.09$, $p = 0.74$) and inclusion of sample data did not improve a linear mixed effect model ($\lambda = 0.22$, $p = 0.64$).

To test the specificity of these effects, we looked at performance in the rats excluded due to incorrect cannula placements. Rats were able to discriminate the novel location both after saline ($t = 2.49$, $p = 0.017$) and APDC infusions ($t = 2.59$, $p = 0.016$) and there was no difference in discrimination scores across drug conditions ($t = -0.43$, $p = 0.67$, $d = -0.15$; Fig. S7).

Finally, we tested whether the effect of local infusions on the consolidation of spatial memory could be generalized to another novelty-driven task, the object-in-place task (Fig. 5g). We found that rats were able to discriminate the displaced objects at test following saline infusions ($t = 3.27$, $p = 2.22 \times 10^{-3}$, one-sided within-subject permutation test Fig. 5h,i), whereas rats performed at chance following APDC infusions ($t = -0.18$, $p = 0.57$, one-sided within-subject permutation test Fig. 5h,i). These drug-related differences were reflected in a significant difference in discrimination scores ($t = 2.13$, $p = 0.024$, $d = 0.46$, one-sided within-subject permutation test Fig. 5h,i). As in the NPP task, this difference was not due to changes in general exploratory behaviors at sample or at test (sample: $t = 0.79$, $p = 0.44$, $d = 0.17$; test: $t = 1.31$, $p = 0.21$, $d = 0.28$; two-sided within-subject permutation tests). While total sample exploration did not relate to discrimination scores at test (saline: $r = -0.06$, $p = 0.81$; APDC: $r = -0.10$, $p = 0.70$; model with sample exploration versus simpler model: $\lambda = 0.22$, $p = 0.64$), object preference at

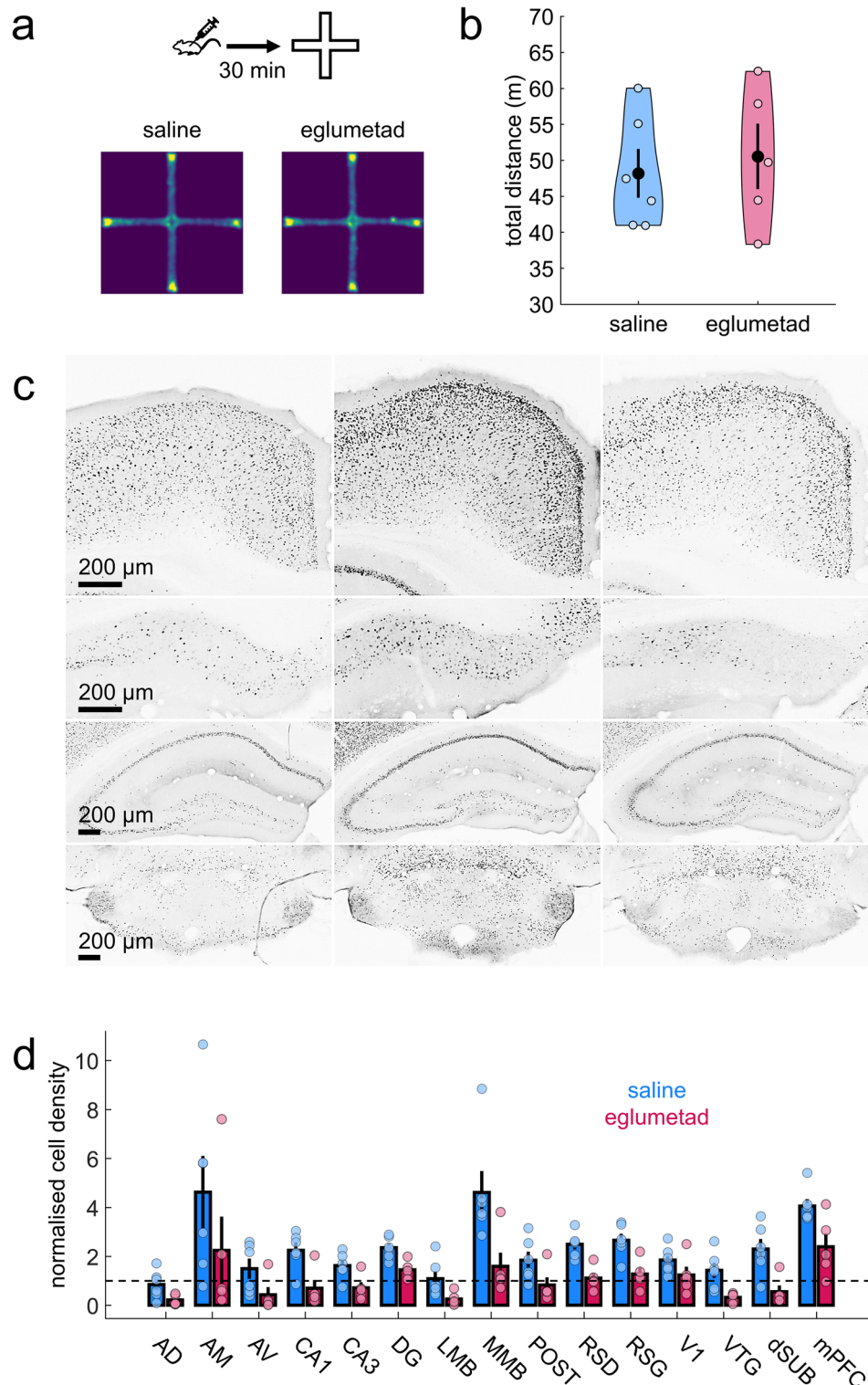


Figure 3. The effect of eglumetad on motility and *c-fos* induction in mice (Experiment 3). **(a)** Heatmaps showing cross-maze motility following saline or eglumetad (10 mg/kg) injections. **(b)** Violin plots representing total distance travelled in cross-maze. Large black dots are mean values, the error bars are standard error of the mean and smaller light dots are data from individual animals (saline: $n = 6$, eglumetad: $n = 5$). **(c)** Representative images of selected areas of the Papez network (from top to bottom: retrosplenial cortex, dorsal subiculum, dorsal hippocampus, mammillary bodies) displaying differences in *c-fos* staining in home-cage controls (first column), mice under saline (second column) and mice under eglumetad (third column). Images from other regions as well as the quantification of home-cage control *c-fos* densities are displayed in Fig. S4. **(d)** Bar chart showing mean regional differences in relative *c-fos* expression (fold density change relative to mean home-cage control values) with counts from mice under saline or eglumetad in blue and red, respectively. The error bars are standard error of the mean and data from individual animals are shown as colored dots. The horizontal line represents no change relative to home-cage control. AD anterodorsal thalamic nucleus, AM anteromedial thalamic nucleus, AV anteroventral thalamic nucleus, CA1/CA3 hippocampal subfields, DG dentate gyrus, LMB lateral mammillary bodies, MMB medial mammillary bodies, POST postsubiculum, RSD dysgranular retrosplenial cortex, RSG granular retrosplenial cortex, V1 primary visual cortex, VTG ventral tegmental nucleus of Gudden, dSUB dorsal subiculum, mPFC medial prefrontal cortex.

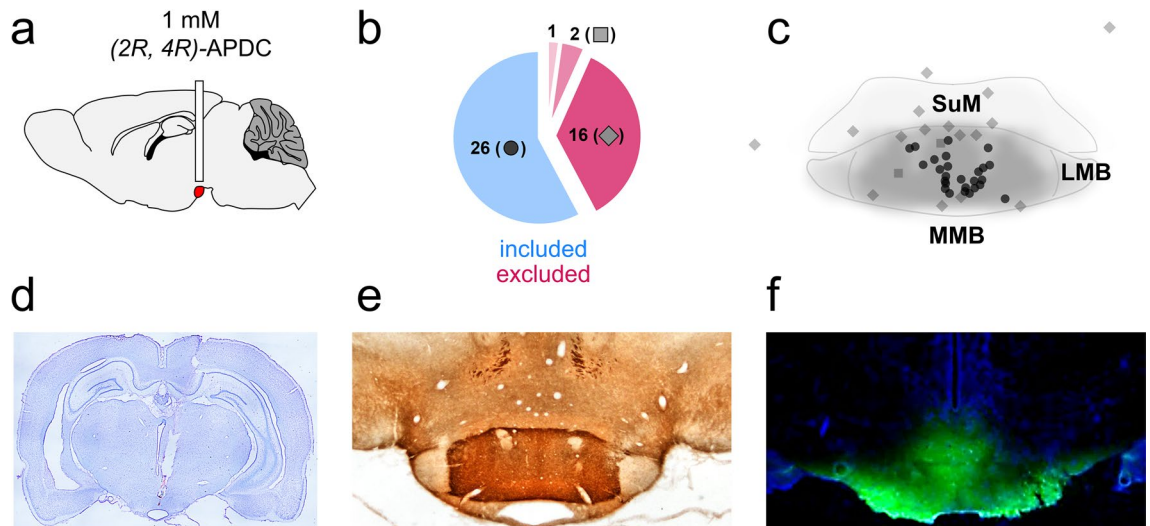


Figure 4. Local drug infusion in the mammillary bodies. (a) Diagrammatic representation of the guide cannula implant. The mammillary bodies are highlighted in red. (b) Subject classification based on histological verification. Out of 45 cannulation surgeries, 26 were classified as successful and 16, unsuccessful. Two animals with good cannula placement were rejected due to excess damage and one animal was removed from the study due to unrelated health issues. (c) Estimated cannula tip positions projected onto a mean mammillary body outline. Note that the average boundaries of the mammillary bodies are only approximated here, see Fig. S5 for individual coronal levels as well as images of cannulated mammillary bodies for all cases. Dots represent successful cannulations, diamonds misplaced cannulations and squares, excess damage (in both b&c). *SuM* supramammillary nucleus, *LMB* lateral mammillary body, *MMB* medial mammillary body. (d) Coronal section (Nissl staining) displaying the guide cannula track and infusion cannula tip location in the mammillary bodies. (e) *mGluR2* immunostaining in the mammillary bodies. The label clearly differentiates the medial mammillary nucleus from the surrounding tissue, including the supramammillary nucleus. (f) the spread of locally infused fluorescent dye (acridine orange) in the mammillary bodies.

sample (sample discrimination scores for subsequently displaced objects) showed a positive relationship with test discrimination scores for rats infused with saline ($r = 0.67$, $p = 0.0035$) but not with APDC ($r = -0.33$, $p = 0.20$). Consistent with this, an interaction model (sample discrimination scores \times drug) offered a better fit compared to a simple model ($\lambda = 10.73$, $p = 0.0047$) and to an additive model ($\lambda = 9.77$, $p = 0.0018$), returning a significant drug \times sample_D2 interaction ($F_{1,30} = 11.31$, $p = 0.0021$) and a main effect of drug ($F_{1,30} = 7.71$, $p = 0.0094$).

Discussion

We identified a role for the mGluR2/3 agonist, eglumetad, in early spatial memory consolidation and this was mediated, in part, by its effect on the medial mammillary bodies. Post-sample administration of mGluR2/3 receptor agonists either injected systemically or infused into the mammillary bodies impaired performance on a novel place preference task. The systemic effects were found to be highly reliable as the same pattern was observed across both mice and rats; in mice the effects were observed in both males and females. mGlu2 receptors are strongly expressed in the Papez network in the rodent brain¹⁹, a brain network important for memory². Consistent with this, we found that systemic injections of eglumetad in mice markedly reduced novelty-induced *c-fos* expression across the Papez network, including the mammillary bodies, hippocampus, retrosplenial cortex and ventral tegmental nucleus of Gudden, indicating an inhibitory effect across this memory network. This pattern of reduced activity replicated findings from a previous glucose imaging experiment³⁰, establishing the impact of mGluR2/3 agonists on limbic memory networks. To determine whether local inhibition of the mammillary bodies could produce a similar behavioral effect to a systemic mGluR2/3 agonist, or whether network-wide changes were necessary, we selectively targeted the mammillary bodies using the mGluR2/3 agonist, 2R, 4R-APDC. A remarkably consistent pattern of findings was observed with the local manipulation as with the systemic injections, suggesting the systemic effect of mGluR2/3 agonism was in part driven by its effect on the mammillary bodies. Furthermore, we extended our findings by showing impaired consolidation of a separate behavioral task, the object-in-place task³¹, which is known to be sensitive to lesions of mammillary body pathways³.

Neither systemic administration of an mGluR2/3 agonist, nor selective infusion into the mammillary bodies, affected the overall activity of rats or mice, as measured by open field exploration. Both eglumetad injected mice and locally infused rats showed a tendency to explore the center of the maze more but only according to one measure in each case (mean distance from center for mice and time spent in the center for rats); these trends are consistent with the anxiolytic effect of mGluR2/3 agonists³² but highlight more subtle effects that depend on the measures observed. There was also no difference in animals' overall activity in the test phase of the discrimination tasks, despite impaired performance. This would suggest that the discrimination effects are driven by memory impairments resulting from impoverished consolidation, rather than non-specific changes to activity during the test stage. Consistent with this, the brain occupancy data showed that following systemic administration,

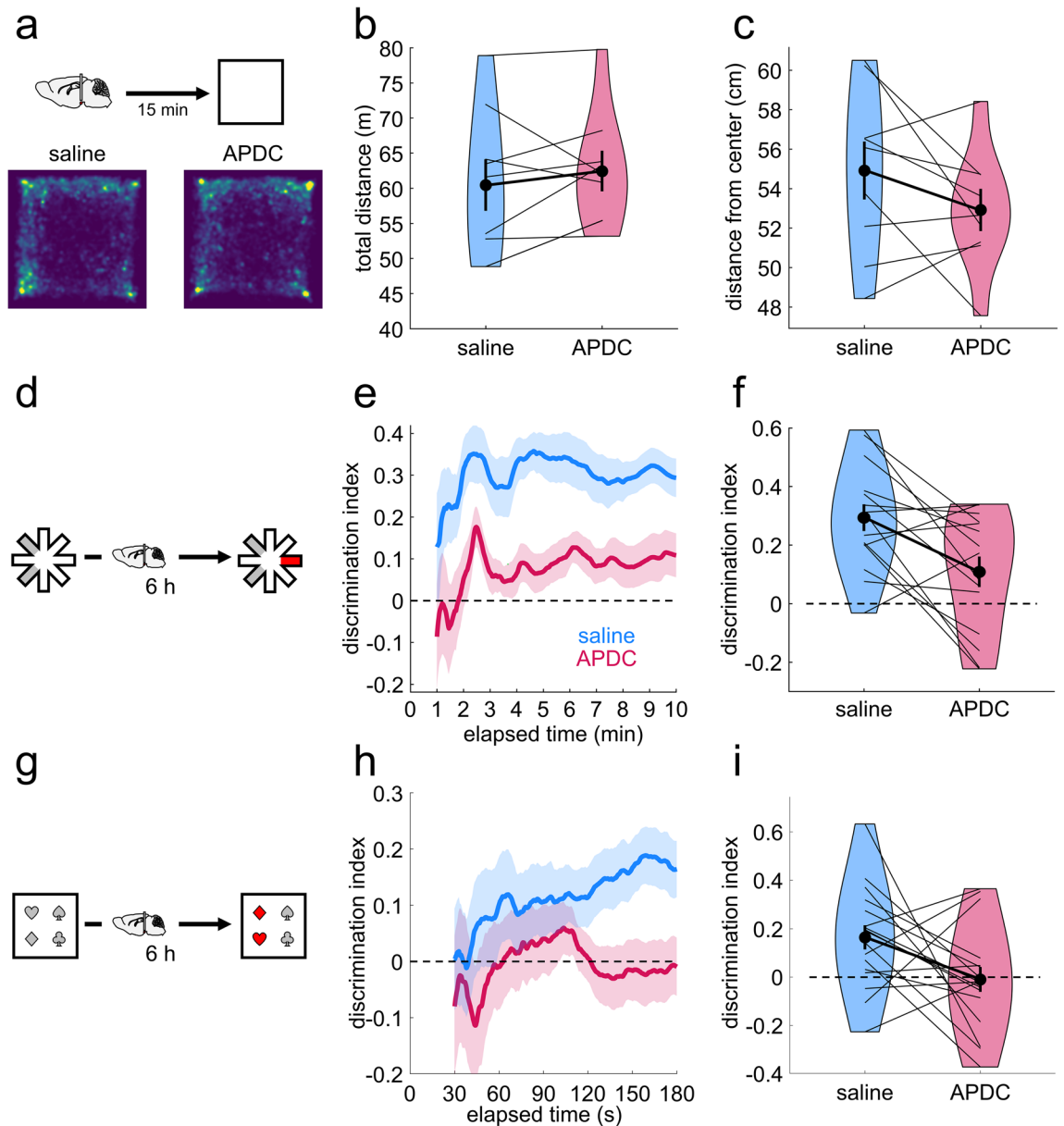


Figure 5. The effect of APDC infusions into the mammillary bodies on open field activity, novel place preference and object-in-place in rats. **(a)** Schematic representation of the open field task and heatmaps representing mean arena occupancy (within-subject $n=9$). **(b)** Violin plot of total distance travelled, as in Fig. 1 b. **(c)** Violin plot of the mean distance from center of the open field. Lower values suggest less anxiety. **(d)** Schematic representation of the NPP task. **(e)** Timeline of the cumulative discrimination index in rats that received saline (blue) or APDC infusions (red) following sample (within-subject design, $n=15$). The solid lines represent mean values and the shaded areas, the standard error of the mean. **(f)** Violin plot of mean discrimination indices, calculated over 10 min of maze exploration at test. **(g)** Schematic representation of the object-in-place task. **(h)** Timeline of the cumulative discrimination index in rats that received saline (blue) or APDC infusions (red) following sample (within-subject design, $n=17$). The solid lines represent mean values and the shaded areas, the standard error of the mean. **(i)** Violin plot of mean discrimination indices, calculated over 10 min of maze exploration at test. The horizontal line in **(e)**, **(f)**, **(g)**, **(i)** denotes chance-level performance.

eglumetad had mostly cleared from the brain after the first hour. As such, the post-sample drug manipulations can be considered in terms of their impact on early consolidation rather than directly affecting the recall stage.

We observed no mean differences in sample activity, as would be expected given the manipulations were carried out after the sample phase. However, we did find relationships between sample activity and test scores at an individual animal level across most of the behavioral tasks, likely driven by animals' biases towards certain objects or maze arms. By including these sample exploration data in the analyses, we were able to reduce some of the variance and better isolate the effect of experimental treatment, making the data more robust and highlighting the potential benefit of using sample data in these types of experiments. The current study employed a two-phase design with a 6-h consolidation window, which capitalized on rats' and mice's natural ultradian activity patterns.

It is unclear whether manipulating the length of the sample-test delay would have produced an equivalent deficit, however, lesions of the mammillary bodies or their principal efferent pathway have been shown to impair performance on the OIP task at shorter delays^{3,33}. Considering the systems-wide impact of eglumetad injections on *c-fos* expression, it might be predicted that that memory storage over longer delays, requiring greater cortical engagement, would also be vulnerable to mGluR2/3 agonist effects.

Almost all previous behavioral studies assessing the role of the mammillary bodies have involved permanent lesions, making it difficult to draw conclusions about their contributions to specific stages of memory processing. One of the few inactivation studies found that manipulation of the mammillary bodies in rabbits immediately after trace conditioning impaired reflex learning. By contrast, there was no effect if inactivation occurred 3 h after training, suggesting a role for the mammillary bodies during the early consolidation period³⁴. Glucose imaging and cytochrome oxidase imaging studies have also shown increased mammillary body activity during the first few hours following task learning^{35–37}, consistent with a role for the mammillary bodies in this early post-encoding period. However, as we only administered mGluR2/3 agonists immediately after the sample phase, further experiments would be needed to determine whether inactivation at later time points produced similar effects.

Temporary inactivation of both dorsal subiculum³⁸ and the anterior thalamic nuclei³⁹, regions that send inputs to, and receive outputs from the mammillary bodies, respectively, have both been shown to affect memory consolidation, suggesting that they, along with the mammillary bodies, form part of an extended consolidation network. Indeed, the mammillary bodies' role in mediating sharp-wave ripple-related activity between the dorsal subiculum and anterior thalamic nuclei might be key to this role in consolidation^{15,40}. However, there are also high expression levels of mGluR2 in the ventral tegmental nucleus of Gudden and, in agreement with this, we found reduced *c-fos* expression in this region following eglumetad injections. Therefore, the reciprocal mammillary body-tegmental nuclei pathway could also be contributing to consolidatory mechanisms, and the behavioral impairments observed.

mGluR2/3 agonists have been identified as a potential treatment for schizophrenia⁴¹. The present results are difficult to interpret in terms of therapeutics since we investigated only the acute effects of drug administration. Chronic administration may produce different results on memory consolidation, with the agonist present at multiple stages of the task. Furthermore, downregulation of receptors and compensatory responses following chronic administration could also produce different effects. Nevertheless, future work into mGluR2-targeting agents as a treatment should consider the impact on the mammillary bodies⁴² and, more generally, the effects on memory processing.

Improving the therapeutic potential of mGluRs requires mechanistic understanding of their roles across multiple brain systems. Our results demonstrate their relevance to long-term spatial memory via interactions within the limbic system and highlight the specific role of the mammillary bodies in early memory consolidation. The effect of systemic eglumetad delivery on *c-fos* expression suggests that the effects on consolidation may be driven by overall depression of neuronal activity. In support of this, group II mGluRs act as glutamate autoreceptors whose activation results in reduced presynaptic glutamate release, as seen in the hippocampus, prefrontal cortex, sensory cortices and others^{43,44}. In the case of the mammillary bodies, mGluR2 is, however, likely to directly exert its function by reducing neuronal excitability postsynaptically²⁹ (although the contribution of presynaptic and astrocytic mGluR2 cannot be ruled out). As such, impaired early consolidation following local drug infusion may simply reflect diminished mammillary body activity levels, thus reducing transmission of theta activity and bursting activity, particularly as mGluR2/3 agonists have been shown to preferentially affect spike frequency^{45,46}.

Together, the present results demonstrate that modulating neural activity in the Papez network, via mGluR2/3 agonism, impacts early memory consolidation. Furthermore, mammillary body inhibition is sufficient to produce similar effects to those seen following systemic injections, highlighting the mammillary bodies as a vital node for consolidation. Given the mammillary bodies are affected in several neurological and psychiatric disorders^{42,47–53}, this gives a greater understanding of some of the mechanisms via which disruption to the mammillary bodies can impact cognitive processing.

Materials and Methods

Animals

Rats

A total of 73 male Lister Hooded rats (Envigo, UK) were used in the study: Experiment 1 involved 28 animals (~320–360 g at the time of injections); Rat Experiment 3 combined 45 rats from across three separate cohorts. Rats were housed in pairs in standard large cages (Rat Experiments 1 and 2) or large Double Decker cages (Experiment 3, Tecniplast, UK) with enrichment (chewsticks, tunnels) in a temperature-controlled room with a 12 h light/dark cycle. Prior to behavioral testing, all rats were food restricted to a minimum of 85% of their free-feeding weight. Water was available ad libitum throughout.

Mice

A total of 51 c57bl6/j mice were used: Experiment 2 included 33 mice (15–25 weeks old at the start of the experiment, 15 female, 21 bred in-house and 12 sourced from Charles River, UK); Experiment 3 included 18 mice (21–29 weeks of age at the start of the experiment, three female, all bred in-house). Mice were housed in groups of two, in a temperature-controlled room, with enrichment (chewsticks, tunnels), under a 12 h light/dark cycle and with ad libitum access to food and water.

All experiments were performed in accordance with the UK Animals (Scientific Procedures) Act, 1986 and associated guidelines, the EU directive 2010/63/EU, as well as the Cardiff University Biological Standards Committee; experimental protocols were approved by the Cardiff University Biological Standards Committee and the UK Animals in Science Regulation Unit. The experiments were reported according to the ARRIVE guidelines.

Randomization and blinding

For all experiments, test parameters (e.g. arm numbers, object pairs) were counterbalanced by pseudo-randomization (Latin cross method) such that each drug treatment condition received an equivalent experience. Drug administration schedules were also pseudo-randomized so that each testing day comprised vehicle and drug delivery in a roughly 50/50 ratio. For mouse experiments, the different sexes were tested on separate days when possible. Experimenters were not always blind to the drug condition while running the tasks, however, there were no direct experimenter-animal interaction once the animals commenced the tasks; drug assignments were blinded at the analysis and scoring stages. For histological analyses (*c-fos* region of interest selection, cannula placement validation), as well as case exclusion based on aberrant behavioral profiles, the identity of the animals or drug assignment or test performance were obscured such that they could not inform the decisions.

Experiment 1

Rats were subject to two behavioral testing paradigms: the open field and the novel place preference (NPP). The open field task was employed to rule out drug effects on overall activity whereas the NPP task tested the effect of the drug on memory consolidation.

For open field, 8 rats were first habituated to the apparatus over three 10 min sessions. The testing arena was a square, opaque wooden box (100 × 100 × 42 cm high) lined with sawdust, located on the floor of an evenly illuminated room (280 × 295 × 260 cm high). As it was a within-subject experiment, rats were tested on two separate days, approximately one week apart, receiving either eglumetad (6 mg/kg, 10.8 mM; also known as LY-354740, Tocris, UK) or saline vehicle injections, according to a counterbalanced design. Thirty mins after injections, rats were placed in the center of the open field arena for 10 min (morning session). Rats were returned to their home cages and again exposed to the open field for 10 min, 6 h after the morning open field session (afternoon session). Animals were recorded with an overhead camera (GoPro Silver 7, GoPro Inc., USA) while performing the task.

The NPP task was run in a modified radial arm maze. The maze comprised a central arena (35 diameter × 25 cm high) and eight radiating arms (10 × 87 × 18 cm high), raised 68 cm off the floor. The base of the maze was white and opaque whereas the walls of the maze were made of clear Perspex. Arm entrances were blocked off by transparent doors operated remotely by the experimenter. The tops of the arms were covered by transparent plastic sheets to prevent the rats from climbing out. A translucent foil collar was also placed around the top of the central arena to discourage rats from climbing. The maze was positioned in the center of a room (255 × 330 × 260 cm high) and was surrounded by white curtains. The room was dimly lit by partially covered fluorescent batten lightbulbs affixed to the ceiling. Task performance was captured with a camera (GoPro Silver 7, GoPro Inc., USA) mounted on a boom pole above the maze.

All animals received 3–4 habituation sessions prior to testing. For habituation, rats were individually placed in the center platform for 30 s after which two of the eight doors were opened and the rats were allowed to freely explore for 10 min. The two habituation arms formed a linear track and were kept the same for each rat across habituation sessions.

Each trial comprised a sample and a test phase, 6 h apart. the testing room was re-configured for each trial: Curtains were decorated with ~ 12 novel three-dimensional landmarks (e.g. Christmas decorations) and the center of the maze was sprayed with a novel baking aroma (e.g. vanilla, caramel, lemon, mint). This was to provide a novel context for each trial to maintain the animals' interest. During sample runs, animals were given access to a previously unexplored set of arms 90° apart (see Fig. 1d). As with habituation, animals were first placed in the center arena for 30 s and then allowed to enter the two novel arms for another 10 min. Rats received intraperitoneal injections of eglumetad or saline vehicle immediately after the sample phase. They were then returned to their home cages, which were placed in a quiet room for 6 h until test. The test phase involved animals having access to the same two arms as in the sample phase as well as access to a third novel arm at 135° from either sample arm see Fig. 1d). This additional arm was considered a goal arm, i.e., if animals remember the two arms from the sample phase, the goal arm should be relatively more novel and therefore more interesting. Habituation and trial arms were assigned to each rat in a pseudo-randomized, counterbalanced fashion, and the experiment was run according to a within-subject design such that each rat received both injection types on separate occasions, at least 7 days apart.

Drug occupancy

Rats were given intraperitoneal injections of eglumetad before being returned to their home cage for a predetermined amount of time (10 min, 30 min, 1 h, 3 h, 6 h). The animals were killed by a rising concentration of CO₂, followed by decapitation, and the brains were rapidly removed using bone scissors and forceps. A slice of brain was excised using a razor and weighed (each slice was between 100 and 150 mg for ease of homogenization), then placed inside an Eppendorf tube on dry ice. The brain samples were thawed on wet ice and ice cold 10 mM KH₂PO₄ buffer (pH = 7) was added to the tube at a 1 mg:9 ml ratio of brain sample to buffer. An electronic homogenizer was used to generate a smooth solution. The homogenized samples were then stored at – 80 °C until further processing.

Standard curve preparation. Seven 1:3 serial dilutions of a 10 mM dimethylsulfoxide(DMSO) stock were made, yielding an eight-point Standard Curve (SC) with the following concentrations (mM): 1, 0.33, 0.11, 0.037, 0.012, 0.0041, 0.0013, 0.00045. 1 µL of each SC dilution were dispensed into separate wells of one column of a deep well (1 mL) 96-well polypropylene plate (Phree, Phenomenex, USA). 100 µL untreated homogenized brain was aliquoted into each well (giving final concentrations of 10, 3.3, 1.1, 0.37, 0.123, 0.041, 0.0137 and 0.0045 µM), then mixed and incubated at room temperature for 10 min. 300 µL of a quench solution (10 mL MeOH + 10 µL 0.1 mM carbamazepine (internal standard) DMSO stock; [final] = 0.1 µM) was added to each well

and mixed. A further 600 μL MeOH was added to each well and mixed gently. The plate(s) were then centrifuged at 4000 rpm for 30 min to pellet the precipitate. The supernatant (approximately 850 μL) was then transferred into separate wells of a HybridSPE-plus 96 well filter plate (Sigma, Japan).

Sample preparation. 100 μL of each homogenized brain sample was placed into separate wells of a deep well (1 mL) 96-well polypropylene plate (Phree, Phenomenex, USA). 300 μL of quench solution was then added to each sample and mixed. A further 600 μL of MeOH was added to each well and mixed gently. The plates were then centrifuged at 4000 rpm for 30 min to pellet the precipitate. The supernatant (approximately 850 μL) was then transferred into separate wells of a lipid HybridSPE-plus 96 well filter plate (Sigma, Japan) taking care not to disturb the pellet.

Filtration. Experiment and standard curve samples were filtered under vacuum into a fresh 1 mL deep well, 96 well plate and placed in a vacuum concentrator (SPD120 SpeedVac Vacuum Concentrator, Thermofisher, USA). The vacuum evaporation was run for 5 h at 50°C after which the plate was incubated overnight at room temperature. All dried samples were re-suspended in 150 μL 50% MeCN. All experimental and standard curve samples were then placed on a 96 well polypropylene plate before being sealed with a 'zone-free' sealing film (Alpha Laboratories, cat # ZAF-PE-50, UK) for LC/MS-MS sampling and analysis (see Supplementary Materials). All samples were analyzed in duplicate.

mGluR2 Immunohistochemistry

We used previously frozen/cryoprotected archival rat tissue, cut at 30 μm . Tissue was washed in PBST (0.2% Triton-X in PBS), then transferred to an EDTA buffer for 20 min at 80 °C, followed by a further 20 min at room temperature. Endogenous peroxidase activity was blocked by incubation in 3% hydrogen peroxidase solution in methanol and unspecific binding blocked by a two-hour incubation in 3% normal horse serum (NHS) in PBST (0.2% Triton-X in PBS). Sections were incubated in mGluR2 mouse monoclonal antibody (1:500, Santa Cruz, USA, sc-271655, in PBST with 1% NHS) overnight at 4 °C followed by a 2 h incubation in horse anti-mouse biotinylated secondary (1:200, Vector, 2BScientific, UK, BA-200 in PBST with 1% NHS). The signal was amplified with an ABC kit (PK-6101 VectaStain kit, 2BScientific, UK) and developed by chromogenic peroxidase reaction (DAB Substrate Kit, 2BScientific, UK), all according to manufacturer's instructions. Tissue sections were mounted, dehydrated, and cleared in xylene prior to coverslipping and imaging.

Experiment 2

As with Experiment 1, mice were injected with either eglumetad or saline and tested on the open field and NPP paradigms in partially overlapping cohorts of 22 and 26 mice, respectively.

For open field, all mice first received three 10 min habituation sessions to the apparatus (40 cm \times 40 cm, white opaque square box), followed by the test session. At test, animals were injected with saline or eglumetad 30 min prior to being placed in the arena. Animals were allowed to explore the arena for 10 min and their behavior was recorded (USBFHD01M-SFV, ELP, UK). The test was carried out according to a between-subject design in a counterbalanced manner, considering injection type and the sex of the mice.

For NPP, prior to commencing the task, mice were given a minimum of three sessions to habituate them to handling and the experimental room. The task was conducted in a translucent string-and-pulley operated 8-arm radial maze (arm dimensions: length, 36 cm; width, 9 cm; height, 17 cm). The maze was positioned 100 cm above the ground and evenly illuminated by ambient light. An overhead camera (USBFHD01M-SFV, ELP, UK) was used to record behavior. The maze was surrounded by laboratory equipment (sink, fridges, recording stages), serving as visual reference cues. The task was conducted in an analogous manner to that in rats in Experiment 1 except mice did not receive odor cues or additional spatial cues (due to the between-subject design, the mice were only run once on the task so additional cues were not needed to differentiate between test sessions) and were not habituated to the maze prior to the task as in⁵⁴.

Experiment 3

We studied the effect of intraperitoneal eglumetad injections on regional brain activity by utilizing experience-driven *c-fos* induction. Prior to the experiment, mice were habituated to the experimenter and the experimental room over three one-hour sessions involving gentle handling and placement of the home cages in the experimental room. *c-fos* expression was induced by allowing mice to individually explore a novel cross-maze (arm length: 33.5 cm, arm height: 4 cm, arm width: 8 cm; made from clear Perspex, placed 64 cm from the ground) for 10 min each. The animals' behavior was recorded using an overhead camera (USB3MP01H-BFV, ELP, UK). Six mice were injected with eglumetad and six with saline vehicle, 30 min prior to cross-maze exploration, while another six mice remained in their home cages to serve as controls. Following maze exploration, mice were returned to their home cages and euthanized 90 min later with pentobarbital overdose⁵⁵. Mice underwent intracardial perfusion fixation (4% paraformaldehyde (PFA) in phosphate-buffered saline (PBS)). The brains were subsequently removed and fixed for a further 2 h in PFA followed by a 48 h incubation in 25% sucrose solution in PBS. The brains were then trimmed using a custom 3D-printed mould (courtesy of Peter Watson, Biosi, Cardiff University) and sectioned at 35 μm using a sliding stage microtome (Bright Instruments, UK). The tissue was cryopreserved at -20 °C in an ethylene glycol-PBS solution until required.

For each brain region of interest, 6–8 sections were processed per mouse. Endogenous peroxidase activity was blocked by incubation in 3% hydrogen peroxidase solution in methanol and unspecific binding blocked by a two-hour incubation in 3% normal goat serum (NGS) in PBST (0.2% Triton-X in PBS). *c-fos* was detected with a rabbit monoclonal antibody (1:2,500, 9F6, Cell Signaling Technology, USA) in 1% NGS-containing PBST

(incubation solution) for 72 h at 4 °C, followed by two-hour incubation in biotinylated goat anti-rabbit IgG in the incubation solution (1:200, PK-6101 VectaStain kit, 2BScientific, UK) at room temperature, amplified with an ABC kit (PK-6101 VectaStain kit, 2BScientific, UK) and developed by chromogenic peroxidase reaction with nickel enhancement (DAB Substrate Kit, 2BScientific, UK), all according to manufacturer's instructions. Tissue sections were mounted, dehydrated, and cleared in xylene prior to coverslipping and imaging.

Whole-section images were obtained using an automated slide scanner (Olympus VS200, Olympus Life Science, Japan), at 4× magnification. The images were loaded into QuPath (v0.4.3⁵⁶) and *c-fos*-expressing nuclei were automatically detected with a custom script using an image classifier (accuracy: 92%, precision: 92%, recall: 94%) trained on a subset of manually annotated sections within a predetermined set of regions of interest (ROIs). The ROIs included the medial prefrontal cortex (mPFC, combined prelimbic and infralimbic cortex), anterodorsal thalamic nucleus (AD), anteromedial thalamic nucleus (AM), anteroventral thalamic nucleus (AV), dorsal hippocampal regions: CA1, CA3 & DG, lateral (LMB) and medial mammillary body (MMB), postsubiculum (POST), granular (RSG) and dysgranular retrosplenial cortex (RSD), primary visual cortex (V1), ventral tegmental nucleus of Gudden (VTG, its *c-fos*-expressing, ventromedial part only) and dorsal subiculum (dSUB). The number of *c-fos*-positive nuclei was normalized to the area of detection (as density) and mean density values per ROI were computed for each experimental subject.

Experiment 4

To determine the extent to which inhibition of the mammillary bodies alone, via an mGluR2/3 agonist, would impact on memory consolidation, we implanted rats with infusion cannulae and delivered the drug locally. All surgeries were performed under isoflurane anesthesia (induction 5%, maintenance 2%–2.5% isoflurane). At the time of surgery, rats weighed 256–320 g. The animals were positioned in a stereotaxic frame (David Kopf Instruments, USA) and the incisor bar adjusted to achieve a flat skull. For analgesic purposes, 0.1 ml of a 50–50 mixture of lidocaine (20 mg/ml solution, Fresenius Kabi, UK) and bupivacaine (2.5 mg/ml solution, Aspen Pharma, Ireland) was applied topically to the scalp and 0.05 ml Metacam (5 mg/ml, Boehringer Ingelheim UK) was given subcutaneously. The scalp was incised to expose the skull and a craniotomy on the right side was made. The stereotaxic arm was set at 12° towards the midline and a single 8 mm guide cannula (Plastics One, 26 gauge, USA) targeting the medial mammillary bodies was implanted. The stereotaxic coordinates of the implant relative to bregma were anteroposterior – 4.45 mm and lateral – 1.95 mm. The cannula was lowered to – 6.85 mm from the top of the cortex. The implant was anchored to the skull with four screws (SFE-M1.4–3-A2, Accu, UK) and held in place by bone cement (Zimmer Biomet, USA). To prevent blockages, a removable 'dummy' cannula (Plastics One, USA) was inserted into the guide cannula. The anterior and posterior ends of the incision were closed with sutures and the antibiotic powder Clindamycin (Pfizer, USA) was applied topically to the site. To recover, rats were given subcutaneous glucose-saline injections (5 ml) and placed in a heated chamber. This was followed by close post-operative monitoring with ad libitum food access for at least a week. Behavioral testing began 2–3 weeks from surgery.

Implanted rats underwent the open field and NPP tasks, as described for Experiment 1. For open field, rats received the drug infusion 15 min prior to testing. There was no afternoon open field session. For NPP, the drug infusion followed immediately after sample and the animals were tested 6 h later. In addition to these tasks, animals in Experiment 4 were also tested on the object-in-place (OIP) task, which also probed the role of the mammillary bodies in memory consolidation, this time utilizing object-place relationships.

For OIP, animals were tested in a gray square wooden arena (100 × 100 × 42 cm high) with a clear acrylic lid. The floor of the arena was covered in a layer of sawdust. A cue card featuring geometric shapes was affixed to one wall of the arena to provide a polarizing cue. Additional salient visual cues, such as geometric shapes and high contrast stimuli, were attached to the walls of the testing room (280 × 295 × 260 cm high). Behavior was recorded using an overhead-mounted action camera (GoPro Silver 7, GoPro Inc, USA). The test objects were complex 3-dimensional shapes constructed from Duplo (Lego, Denmark) that varied in color and size (16 × 16 × 14 cm high–15 × 16 × 19 cm high) and were too heavy to displace (each set comprised a red, a green, a blue and a yellow object). There were duplicates of each set of objects such that each test session used a different object set and within a session and duplicates were used for test and sample. Prior to testing, rats received five habituation sessions over 3 days. On the first day, rats were placed into the arena in home cage pairs for 10 min in the morning and 10 min in the afternoon. The following day, rats received two 5 min sessions individually. On the last day, individual rats received a single 5 min session. No objects were present in the arena during habituation. On test days, the task involved a sample and a test phase, separated by a 6 h delay. One object was placed in each corner of the arena, positioned 10 cm from the wall. An individual rat was transported to the room in a metal carrying box with a lid to prevent them from seeing outside the box. In the sample phase, the animal was placed in the center of the arena and allowed to explore the objects for 5 min. The rat was then individually placed in a holding cage in a quiet room for the delay period. For the 3 min test phase, identical duplicate objects were used but two of the objects swapped locations. All objects were cleaned with 70% ethanol between animals to remove odor cues and sawdust. The set of objects, the object pair that changed location, and object corner positions were counterbalanced across animals. As it was a within-subject design, all rats were tested twice, once under APDC and once under saline, this was also counterbalanced across animals. There was a minimum 7-day interval between the test sessions to maintain interest in the task.

At the conclusion of Experiment 4, all rats were given an overdose of pentobarbital and transcardially perfused. In some cases, we infused a fluorescent dye, acridine orange (11504047, Invitrogen, UK), to help estimate the spread of the drug infusate (Fig. 4f). Extracted brains were post-perfused in PFA for 3 h, incubated in 25% sucrose solution for 12–24 h and cut at 40 μm on a sliding-stage microtome (Bright Instruments, UK). Mounted and dehydrated sections (1-in-4 series) were counterstained with cresyl violet to help visualize the cannula

tracks. We also attempted to measure *c-fos* signal as in Experiment 3, however, we found cannulations produced very strong staining artifacts. While the tissue was not suitable for *c-fos* analysis, it was beneficial for identifying cannula placements (Fig. S4b). Brain sections were imaged using an automated slide scanner (VS200, Olympus, Japan) at 4× magnification and independently assessed by three experienced researchers blinded to the behavioral data. Cases deemed acceptable by all three researchers were included in analyses. Reasons for exclusion included: (a) placement of cannula tip outside the borders of the medial mammillary nucleus, including the supramammillary nucleus, (b) cannula tip bordering the third ventricle/outer edge of the mammillary bodies, (c) excess mechanical damage. Included cases were centered on the medial part of the medial mammillary nucleus, leaving laterally adjacent structures, including the tuberomammillary nuclei, unaffected.

Drug administration

The drugs eglumetad (also known as LY-354740, Tocris, UK) and 2R, 4R-APDC (Tocris, UK, abbreviated to 'APDC' hereafter) were administered via intraperitoneal injection or via local brain infusion, respectively. We used APDC for local infusions as its efficacy at inhibiting mammillary bodies has been demonstrated in slice recordings²⁹. However, since APDC does not readily cross the blood–brain barrier, we used its analogue, eglumetad, for systemic injections^{57,58}. Injections/infusions were preceded by habituation to gentle restraint, typically over 3 sessions.

For intraperitoneal eglumetad injections, mice received 10 mg/kg (at 360 μM in saline, *pH*-adjusted to within 7.0–7.4) whereas rats, 6 mg/kg (at 10.8 mM in saline, *pH*-adjusted to within 7.0–7.4) of the drug solution (a 30 g mouse would therefore receive 450 μL of solution whereas a 300 g rat, 900 μL of solution). A lower dose was used in rats based on pilot data suggesting motor impairments at higher doses. Saline was used as the vehicle control.

For infusions, rats received 0.6 μL of APDC (at 1 mM in distilled water), *pH*-adjusted to 7.0–7.4 or saline. Animals were lightly restrained, and the internal 'dummy' cannula was replaced by an infusion cannula (Plastics One, 33-gauge) that projected 2 mm below the tip of the guide cannula. The infusion cannula was connected via polyethylene tubing to a 10 μL Hamilton syringe mounted on an infusion pump (Harvard Apparatus, USA). A volume of 0.6 μL was infused over approximately 2 min (a rate of 250 nL/min). The infusion cannula remained in place for a further 2 min to allow complete diffusion of the infusate. The 'dummy' cannula was re-inserted, and the animal returned to its cage.

Data analysis

Sample sizes for consolidation experiments were informed by pilot data, which indicated that demonstrating a 75% difference in discrimination scores would require around 14 animals in a within-design experiment, given the variance in pilot cohorts. To account for cannula misplacements and case exclusions due to other factors (aberrant behavior, health issues, experimenter error), we aimed for three times as many animals in infusion experiments and twice as many animals in the between-subject mouse experiments. The primary outcome measure that confirmed sufficient sample sizes were tests of above-chance discrimination following vehicle administration.

For the open field task, the trajectories of the animals were computed in DeepLabCut⁵⁹ using custom models trained in-house (for each individual experiment). The coordinates were loaded into Matlab and total distance travelled, mean distance from the center of the maze and time spent in the center of the maze were calculated. The center of the maze was defined as the innermost part of the maze comprising 50% of its total area.

For the NPP task, recordings of the behavioral data were manually scored without knowledge of animal assignment, to provide entry and exit times for each arm visit. Entry to an arm was defined as the full head of the animal crossing the arm threshold, followed by its entire body, while an exit was scored when the full head of the animal crossed the threshold in the opposite direction. Periods of grooming as well as excessive biting or licking of maze walls were annotated and later excluded from analysis (animals did not differ in grooming/biting behavior according to drug). The manual scores were loaded into Matlab. Using custom scripts, the number of arm entries, mean arm visit time, cumulative active exploration (sum of total arm visit times) and a cumulative discrimination index (D2) were computed. The D2 score was calculated as the difference in cumulative time spent visiting the novel arm and the mean cumulative time spent visiting familiar arms over the sum of the cumulative novel arm visit time and the mean cumulative familiar arm visit time. The index therefore ranged from -1 (exclusive preference for familiar arms), through 0 (no preference for novel or familiar arms or chance level performance) to 1 (exclusive preference for the novel arm). Positive scores signified novel place preference. D2 values were plotted as function of exploration time (1–10 min) at 1 s resolution and compared between conditions at 10 min exploration time. Both test and sample phases were analyzed, the former to ensure there were no mean group differences in animal activity levels by chance.

For the OIP task, video recordings were loaded into Matlab. The position of the animal's center of gravity was extracted and assigned to the object it was closest to. The object positions and identities were extracted based on color thresholding. Cropped video frames displaying the animal in proximity to one of the four objects were assembled into a tiff file for manual scoring in FIJI. A custom start-up macro in FIJI was written to enable button-controlled user scoring of the videos in a frame-by-frame manner. This method improves the reliability of data as the experimenter is unaware of object placement in the arena at the time of testing, as well as the experimental status of the animal, thus removing potential bias. A frame was assigned an exploration status if the nose of the animal pointed toward the object and was within 1 cm from the object's border. Instances of biting and licking were not considered object exploration. FIJI-outputted csv files were loaded into Matlab for analysis. Total object exploration and a cumulative discrimination score (D2) were computed. The D2 score was calculated as the difference in exploration times between the displaced and non-displaced objects over the sum of total object exploration time.

For the NPP task, animals were removed from analyses if they spent less than 2 min exploring arms at either sample or test and if they idled in a single arm for longer than 1.5 min as well as in cases where running errors occurred (incorrect arms open, etc.). In total, six rats were excluded based on inadequate exploration levels (Experiment 1: two rats were excluded due to poor sample exploration and two for poor test exploration, one following eglumetad infusion and one following saline infusion; Experiment 4: two rats were excluded due to poor sample exploration). One saline-injected mouse was excluded from Experiment 2 due to inadequate exploration levels at test.

For the OIP tasks, animals were removed from analyses if they failed to explore any of the objects at sample or if they spent less than 30 s exploring the objects at either sample or test and (no animals were rejected based on these criteria).

For open field /cross-maze, animals were removed from analyses if they failed to move (i.e., remained in the corner of the arena or refused to enter arms). One eglumetad-injected mouse from Experiment 3 was removed from analyses on this basis.

Statistical analysis

To test for the effect of drugs on behavioral performance, we utilised permutation tests appropriate to the experimental design (between-subject design: *permutationTest*⁶⁰ or within-subject design: *mult_comp_perm_t1*⁶¹; Supplementary Table 1). We used this approach as permutation testing is nonparametric and calculates exact, rather than estimated, *p*-values. Where assumptions for the equivalent parametric test are met, permutation and parametric hypothesis test probabilities are typically near identical. For experiments testing drug effects on memory, it was hypothesized eglumetad/2R,4R-APDC would lead to poorer performance, therefore one-sided (single-tail) tests were employed. Similarly, in open field experiments, it was hypothesized the drugs would lead to reduced motility and lower anxiety, and one-sided tests were used. Tests investigating whether animals performed above chance levels were also one-tailed since below chance performance is statistically implausible⁶². For any other tests (e.g., total number of arm visits on novel place preference task), we did not hypothesize a specific direction for the effect of the drug, and two-sided tests were used. To estimate the magnitude of the effects, we calculated the effect sizes in the form of Cohen's *d*⁶³, using *computeCohen_d*⁶⁴, adjusted to reflect the small (< 50) sample sizes used in the reported experiments.

For memory consolidation tasks, we also tested whether activity at sample explained the variance in discrimination scores observed at test. Informed by the presence of correlations between some sample metrics and discrimination at test, we built a series of linear mixed effect models (*fitlme*) incorporating total active exploration at sample (both NPP and OIP) or object discrimination (OIP only) as confounding factors. If the addition of sample data significantly improved the model (*compare* function), we also tested for a significant improvement with an interaction term (drug by confound). The most parsimonious model with the best fit was chosen in each case.

For Experiment 3, *c-fos* staining density was transformed to represent fold change from baseline (mean home-cage control regional density values). The following linear mixed effect model (*fitlme*) was built to test for the effect of drug injections on *c-fos* induction levels: 'Density~Drug×Region + (1|Animal)'. Simple effects were investigated in an analogous manner, for each individual ROI ('Density~Drug + (1|Animal)') and the computed regional *p*-values were corrected for with the Benjamini–Hochberg method *fdr_bh* add-on⁶⁵.

Manual scoring of behavioral data was performed by several experienced researchers who were unaware of the animals' experimental status at the time of scoring. To ascertain the robustness of the scores, a sub-sample of the videos was re-scored by another researcher. For the NPP task, we found an interclass correlation coefficient (icc) of 0.90 (CI: 0.78, 0.95); *icc21* function⁶⁶.

All statistical analyses were performed with custom scripts in Matlab (2022b, MathWorks, USA), available upon request. All plots were made with *gramm*⁶⁷ in Matlab and modified in PowerPoint (Microsoft, USA).

Data availability

The datasets generated during the current study as well as code used in analysis are available from the corresponding author on request.

Received: 13 December 2023; Accepted: 29 February 2024

Published online: 12 March 2024

References

- Danet, L. *et al.* Thalamic amnesia after infarct. *Neurology* **85**, 2107. <https://doi.org/10.1212/WNL.0000000000002226> (2015).
- McNaughton, N. & Vann, S. D. Construction of complex memories via parallel distributed cortical-subcortical iterative integration. *Trends Neurosci.* **45**, 550–562. <https://doi.org/10.1016/j.tins.2022.04.006> (2022).
- Nelson, A. J. & Vann, S. D. Mammillothalamic tract lesions disrupt tests of visuo-spatial memory. *Behav. Neurosci.* **128**, 494–503. <https://doi.org/10.1037/bne0000001> (2014).
- Park, K. C. *et al.* Amnesic syndrome in a mammillothalamic tract infarction. *J. Korean Med. Sci.* **22**, 1094–1097. <https://doi.org/10.3346/jkms.2007.22.6.1094> (2007).
- Vann, S. D. & Aggleton, J. P. Evidence of a spatial encoding deficit in rats with lesions of the mammillary bodies or mammillothalamic tract. *J. Neurosci.* **23**, 3506–3514 (2003).
- Wetzel, C. D. & Squire, L. R. Encoding in anterograde amnesia. *Neuropsychologia* **18**, 177–184 (1980).
- Cermak, L. S., Uhly, B. & Reale, L. Encoding specificity in the alcoholic Korsakoff patient. *Brain Lang.* **11**, 119–127 (1980).
- Parkin, A. J. *In Neuropsychology of Memory* (Guildford Press, 1992).
- Squire, L. R. Two forms of human amnesia: An analysis of forgetting. *J. Neurosci.* **1**, 635–640 (1981).
- Atherton, L. A., Dupret, D. & Mellor, J. R. Memory trace replay: The shaping of memory consolidation by neuromodulation. *Trends Neurosci.* **38**, 560–570. <https://doi.org/10.1016/j.tins.2015.07.004> (2015).
- Samanta, A., Alonso, A. & Genzel, L. Memory reactivations and consolidation: Considering neuromodulators across wake and sleep. *Curr. Opin. Physiol.* **15**, 120–127. <https://doi.org/10.1016/j.cophys.2020.01.003> (2020).

12. Klinzing, J. G., Niethard, N. & Born, J. Mechanisms of systems memory consolidation during sleep. *Nat. Neurosci.* **22**, 1598–1610. <https://doi.org/10.1038/s41593-019-0467-3> (2019).
13. Dillingham, C. M. *et al.* Mammillothalamic disconnection alters hippocampocortical oscillatory activity and microstructure: Implications for diencephalic amnesia. *J. Neurosci.* **39**, 6696–6713. <https://doi.org/10.1523/jneurosci.0827-19.2019> (2019).
14. Vann, S. D. Re-evaluating the role of the mammillary bodies in memory. *Neuropsychologia* **48**, 2316–2327. <https://doi.org/10.1016/j.neuropsychologia.2009.10.019> (2010).
15. Dillingham, C. M., Wilson, J. J. & Vann, S. D. Electrophysiological properties of the medial mammillary bodies across the sleep-wake cycle. *BioRxiv* **68**, 1321. <https://doi.org/10.1101/2023.10.30.563083> (2023).
16. Tambini, A. & Davachi, L. Awake reactivation of prior experiences consolidates memories and biases cognition. *Trends Cogn. Sci.* **23**, 876–890. <https://doi.org/10.1016/j.tics.2019.07.008> (2019).
17. Żakowski, W. & Zawistowski, P. Neurochemistry of the mammillary body. *Brain Struct. Funct.* **228**, 1379–1398. <https://doi.org/10.1007/s00429-023-02673-4> (2023).
18. Hou, Y. *et al.* Topographical organization of mammillary neurogenesis and efferent projections in the mouse brain. *Cell Reports* **34**, 108712. <https://doi.org/10.1016/j.celrep.2021.108712> (2021).
19. Ohishi, H., Neki, A. & Mizuno, N. Distribution of a metabotropic glutamate receptor, mGluR2, in the central nervous system of the rat and mouse: An immunohistochemical study with a monoclonal antibody. *Neurosci. Res.* **30**, 65–82. [https://doi.org/10.1016/S0168-0102\(97\)00120-X](https://doi.org/10.1016/S0168-0102(97)00120-X) (1998).
20. Lyon, L. *et al.* Fractionation of spatial memory in GRM2/3 (mGlu2/mGlu3) double knockout mice reveals a role for group II metabotropic glutamate receptors at the interface between arousal and cognition. *Neuropsychopharmacology* **36**, 2616–2628. <https://doi.org/10.1038/npp.2011.145> (2011).
21. Schlumberger, C. *et al.* Effects of a metabotropic glutamate receptor group II agonist LY354740 in animal models of positive schizophrenia symptoms and cognition. *Behav. Pharmacol.* **20**, 56–66. <https://doi.org/10.1097/FBP0b013e3283242f57> (2009).
22. Higgins, G. A. *et al.* Pharmacological manipulation of mGlu2 receptors influences cognitive performance in the rodent. *Neuropharmacology* **46**, 907–917. <https://doi.org/10.1016/j.neuropharm.2004.01.018> (2004).
23. Griebel, G. *et al.* The mGluR2 positive allosteric modulator, SAR218645, improves memory and attention deficits in translational models of cognitive symptoms associated with schizophrenia. *Sci. Rep.* **6**, 35320. <https://doi.org/10.1038/srep35320> (2016).
24. Wolf, D. H. *et al.* Effect of mGluR2 positive allosteric modulation on frontostriatal working memory activation in schizophrenia. *Mol. Psychiatry* **27**, 1226–1232. <https://doi.org/10.1038/s41380-021-01320-w> (2022).
25. Riedel, G., Platt, B. & Micheau, J. Glutamate receptor function in learning and memory. *Behav. Brain Res.* **140**, 1–47. [https://doi.org/10.1016/S0166-4328\(02\)00272-3](https://doi.org/10.1016/S0166-4328(02)00272-3) (2003).
26. Crupi, R., Impellizzeri, D. & Cuzzocrea, S. Role of metabotropic glutamate receptors in neurological disorders. *Front. Mol. Neurosci.* <https://doi.org/10.3389/fnmol.2019.00020> (2019).
27. Nadia, R., Urs, G. & Jeanne, S. Activation of group II metabotropic glutamate receptors promotes LTP induction at schaffer collateral-CA1 pyramidal cell synapses by priming NMDA receptors. *The Journal of Neuroscience* **36**, 11521. <https://doi.org/10.1523/JNEUROSCI.1519-16.2016> (2016).
28. Ahnaou, A., Ver Donck, L. & Drinkenburg, W. H. I. M. Blockade of the metabotropic glutamate (mGluR2) modulates arousal through vigilance states transitions: Evidence from sleep–wake EEG in rodents. *Behav. Brain Res.* **270**, 56–67. <https://doi.org/10.1016/j.bbr.2014.05.003> (2014).
29. Lee, C. C. Inhibition of mammillary body neurons by direct activation of Group II metabotropic glutamate receptors. *Neurotransmitter (Houst)* **3**, e1357 (2016).
30. Lam, A. G., Monn, J. A., Schoep, D. D., Lodge, D. & McCulloch, J. Group II selective metabotropic glutamate receptor agonists and local cerebral glucose use in the rat. *J. Cereb. Blood Flow Metab.* **19**, 1083–1091. <https://doi.org/10.1097/00004647-199910000-00004> (1999).
31. Chao, O. Y., Nikolaus, S., Yang, Y.-M. & Huston, J. P. Neuronal circuitry for recognition memory of object and place in rodent models. *Neurosci. Biobehav. Rev.* **141**, 104855. <https://doi.org/10.1016/j.neubiorev.2022.104855> (2022).
32. David, R. H., Joseph, P. T., James, A. M., Darryle, D. S. & Mary Jeanne, K. Anxiolytic and side-effect profile of LY354740: A potent, highly selective, orally active agonist for group II metabotropic glutamate receptors. *J. Pharmacol. Exp. Ther.* **284**, 651 (1998).
33. Parker, A. & Gaffan, D. Mammillary body lesions in monkeys impair object-in-place memory: Functional unity of the fornix-mammillary system. *J. Cognit. Neurosci.* **9**, 512–521. <https://doi.org/10.1162/jocn.1997.9.4.512> (1997).
34. Gromova, E. A., Plakkhinas, L. A. & Nesterova, I. V. The role of the mammillary complex consolidating memory traces. *Zhurnal Vyshei Nervnoi Deiatelnosti Imeni I P Pavlova* **25**, 372–378 (1975).
35. Sif, J. *et al.* Time-dependent sequential increases in [¹⁴C]2-deoxyglucose uptake in subcortical and cortical structures during memory consolidation of an operant training in mice. *Behav. Neural Biol.* **56**, 43–61. [https://doi.org/10.1016/0163-1047\(91\)90279-y](https://doi.org/10.1016/0163-1047(91)90279-y) (1991).
36. Bontempi, B., Jaffard, R. & Destrade, C. Differential temporal evolution of post-training changes in regional brain glucose metabolism induced by repeated spatial discrimination training in mice: Visualization of the memory consolidation process?. *Eur. J. Neurosci.* **8**, 2348–2360. <https://doi.org/10.1111/j.1460-9568.1996.tb01198.x> (1996).
37. Mendez-Lopez, M., Mendez, M., Sampedro-Piquero, P. & Arias, J. L. Spatial learning-related changes in metabolic activity of limbic structures at different posttask delays. *J. Neurosci. Res.* **91**, 151–159. <https://doi.org/10.1002/jnr.23134> (2013).
38. Melo, M. B. D., Favaro, V. M. & Oliveira, M. G. M. The dorsal subiculum is required for contextual fear conditioning consolidation in rats. *Behav. Brain Res.* **390**, 112661. <https://doi.org/10.1016/j.bbr.2020.112661> (2020).
39. Safari, V. *et al.* Individual subnuclei of the rat anterior thalamic nuclei differently affect spatial memory and passive avoidance tasks. *Neuroscience* **444**, 19–32. <https://doi.org/10.1016/j.neuroscience.2020.07.046> (2020).
40. Skelin, I., Kilianski, S. & McNaughton, B. L. Hippocampal coupling with cortical and subcortical structures in the context of memory consolidation. *Neurobiol. Learn. Mem.* **160**, 21–31. <https://doi.org/10.1016/j.nlm.2018.04.004> (2019).
41. Li, M. L., Hu, X. Q., Li, F. & Gao, W. J. Perspectives on the mGluR2/3 agonists as a therapeutic target for schizophrenia: Still promising or a dead end?. *Prog. Neuropsychopharmacol. Biol. Psychiatry* **60**, 66–76. <https://doi.org/10.1016/j.pnpbp.2015.02.012> (2015).
42. Milczarek, M. M., Gilani, S. I. A., Lequin, M. H. & Vann, S. D. Reduced mammillary body volume in individuals with a schizophrenia diagnosis: An analysis of the COBRE data set. *Schizophrenia* **9**, 48. <https://doi.org/10.1038/s41537-023-00376-7> (2023).
43. Petralia, R. S., Wang, Y. X., Niedzielski, A. S. & Wenthold, R. J. The metabotropic glutamate receptors, MGLUR2 and MGLUR3, show unique postsynaptic, presynaptic and glial localizations. *Neuroscience* **71**, 949–976. [https://doi.org/10.1016/0306-4522\(95\)00533-1](https://doi.org/10.1016/0306-4522(95)00533-1) (1996).
44. Jin, L. E. *et al.* mGluR2/3 mechanisms in primate dorsolateral prefrontal cortex: Evidence for both presynaptic and postsynaptic actions. *Mol. Psychiatry* **22**, 1615–1625. <https://doi.org/10.1038/mp.2016.129> (2017).
45. Keele, N. B., Neugebauer, V. & Shinnick-Gallagher, P. Differential effects of metabotropic glutamate receptor antagonists on bursting activity in the amygdala. *J. Neurophysiol.* **81**, 2056–2065. <https://doi.org/10.1152/jn.1999.81.5.2056> (1999).
46. Kintscher, M., Breustedt, J., Miceli, S., Schmitz, D. & Wozny, C. Group II metabotropic glutamate receptors depress synaptic transmission onto subicular burst firing neurons. *PLoS One* **7**, e45039. <https://doi.org/10.1371/journal.pone.0045039> (2012).
47. Molavi, M., Vann, S. D., de Vries, L. S., Groenendaal, F. & Lequin, M. Signal change in the mammillary bodies after perinatal asphyxia. *AJNR. Am. J. Neuroradiol.* **40**, 1829–1834. <https://doi.org/10.3174/ajnr.A6232> (2019).

48. Meys, K. M. E., de Vries, E., Groenendaal, F., Vann, S. & Lequin, M. H. The mammillary bodies: A review of causes of injury in infants and children. *AJNR. Am. J. Neuroradiol.* <https://doi.org/10.3174/ajnr.A7463> (2022).
49. Lequin, M. H. *et al.* Mammillary body injury in neonatal encephalopathy: A multicentre, retrospective study. *Pediatr. Res.* <https://doi.org/10.1038/s41390-021-01436-3> (2021).
50. Connaughton, M. *et al.* The limbic system in children and adolescents with attention-deficit/hyperactivity disorder: A longitudinal structural MRI analysis. *Biol. Psychiatry Glob. Open Sci.* <https://doi.org/10.1016/j.bpsgos.2023.10.005> (2023).
51. Denby, C. E. *et al.* The frequency and extent of mammillary body atrophy associated with surgical removal of a colloid cyst. *AJNR. Am. J. Neuroradiol.* **30**, 736–743. <https://doi.org/10.3174/ajnr.A1424> (2009).
52. Bernstein, H. G. *et al.* A postmortem assessment of mammillary body volume, neuronal number and densities, and fornix volume in subjects with mood disorders. *Eur. Arch. Psychiatry Clin. Neurosci.* **262**, 637–646. <https://doi.org/10.1007/s00406-012-0300-4> (2012).
53. Küçükerden, M. *et al.* Compromised mammillary body connectivity and psychotic symptoms in mice with di- and mesencephalic ablation of ST8SIA2. *Transl. Psychiatry* **12**, 51. <https://doi.org/10.1038/s41398-022-01816-1> (2022).
54. Nicole, O. *et al.* Soluble amyloid beta oligomers block the learning-induced increase in hippocampal sharp wave-ripple rate and impair spatial memory formation. *Sci. Rep.* **6**, 22728. <https://doi.org/10.1038/srep22728> (2016).
55. Morgan, J. I., Cohen, D. R., Hempstead, J. L. & Curran, T. Mapping patterns of c-fos expression in the central nervous system after seizure. *Science* **237**, 192–197. <https://doi.org/10.1126/science.3037702> (1987).
56. Bankhead, P. *et al.* QuPath: Open source software for digital pathology image analysis. *Sci. Rep.* **7**, 16878. <https://doi.org/10.1038/s41598-017-17204-5> (2017).
57. Flor, P. J., Battaglia, G., Nicoletti, F., Gasparini, F. & Bruno, V. Neuroprotective activity of metabotropic glutamate receptor ligands. *Adv. Exp. Med. Biol.* **513**, 197–223. https://doi.org/10.1007/978-1-4615-0123-7_7 (2002).
58. Poli, A. *et al.* Group II metabotropic glutamate receptors regulate the vulnerability to hypoxic brain damage. *J. Neurosci.* **23**, 6023–6029. <https://doi.org/10.1523/jneurosci.23-14-06023.2003> (2003).
59. Mathis, A. *et al.* DeepLabCut: markerless pose estimation of user-defined body parts with deep learning. *Nat. Neurosci.* **21**, 1281–1289. <https://doi.org/10.1038/s41593-018-0209-y> (2018).
60. Krol, L. R. Permutation Test <https://github.com/lrkrol/permutationTest> GitHub. Retrieved 13 November 2023 (2023).
61. Groppe, D. mult_comp_perm_t1(data,n_perm,tail,alpha_level,mu,reports,seed_state) https://www.mathworks.com/matlabcentral/fileexchange/29782-mult_comp_perm_t1-data-n_perm-tail-alpha_level-mu-reports-seed_state MATLAB Central File Exchange. Retrieved 13 November 2023 (2023).
62. Akkerman, S., Prickaerts, J., Steinbusch, H. W. M. & Blokland, A. Object recognition testing: Statistical considerations. *Behav. Brain Res.* **232**, 317–322. <https://doi.org/10.1016/j.bbr.2012.03.024> (2012).
63. Cohen, J. *Statistical Power Analysis for the Behavioral Sciences 2 Edition* (Lawrence Erlbaum Associates Publishers, 1988).
64. Bettinardi, R. G. computeCohen_d(x1, x2, varargin) https://www.mathworks.com/matlabcentral/fileexchange/62957-computecoh_en_d-x1-x2-varargin, MATLAB Central File Exchange Retrieved 13 November 2023 (2023).
65. Groppe, D. fdr_bh https://www.mathworks.com/matlabcentral/fileexchange/27418-fdr_bh MATLAB Central File Exchange Retrieved 13 November 2023 (2023).
66. Zoeller, T. Intraclass correlation coefficient with confidence intervals <https://www.mathworks.com/matlabcentral/fileexchange/26885-intraclass-correlation-coefficient-with-confidence-intervals> MATLAB Central File Exchange Retrieved 14 November 2023 (2023).
67. Morel, P. Gramm: Grammar of graphics plotting in Matlab. *J. Open Source Softw.* **3**(23), 568. <https://doi.org/10.21105/joss.00568> (2018).

Acknowledgements

This research was funded by the Wellcome Trust (Wellcome Trust Senior Research Fellowship awarded to SDV (WT212273/Z/18). For the purpose of Open Access, the author has applied a CC BY public copyright licence to any Author Accepted Manuscript version arising from this submission. SH is funded by a BBSRC PhD studentship. Thanks to Marcus Hanley from the Medicines Discovery Institute, Cardiff University, for carrying out brain occupancy analyses and to Peter Watson from BIOSI, Cardiff University for help with 3D printed brain matrices.

Author contributions

M.M. and J.P. performed the surgeries. M.M., J.P., T.H., S.H., E.A. carried out data collection and behavioral scoring. M.M. wrote the code for data analysis, prepared the figures and carried out statistical analyses. M.M., J.P. and S.V. wrote the main manuscript text. All authors reviewed the manuscript.

Competing interests

The authors declare no competing interests.

Additional information

Supplementary Information The online version contains supplementary material available at <https://doi.org/10.1038/s41598-024-56015-3>.

Correspondence and requests for materials should be addressed to S.D.V.

Reprints and permissions information is available at www.nature.com/reprints.

Publisher's note Springer Nature remains neutral with regard to jurisdictional claims in published maps and institutional affiliations.



Open Access This article is licensed under a Creative Commons Attribution 4.0 International License, which permits use, sharing, adaptation, distribution and reproduction in any medium or format, as long as you give appropriate credit to the original author(s) and the source, provide a link to the Creative Commons licence, and indicate if changes were made. The images or other third party material in this article are included in the article's Creative Commons licence, unless indicated otherwise in a credit line to the material. If material is not included in the article's Creative Commons licence and your intended use is not permitted by statutory regulation or exceeds the permitted use, you will need to obtain permission directly from the copyright holder. To view a copy of this licence, visit <http://creativecommons.org/licenses/by/4.0/>.

© The Author(s) 2024